Supporting Information:

Tuning the Selectivity of Biomass Oxidation over Oxygen Evolution on NiO-OH Electrodes

Laxman Gouda,[a,b] Laurent Sévery,[a] Thomas Moehl,[a] Elena Mas-Marzá,[b] Pardis Adams,[a] Francisco Fabregat-Santiago*[,b] and S. David Tilley*[,a]

[a] Department of Chemistry, University of Zurich, Winterthurerstrasse 190, CH-8057 Zurich Switzerland

[b] Institute of Advanced Materials (INAM), Universitat Jaume I, Avda. V. Sos Baynat s/n, 12006 Castelló de la Plana, Spain.

1. EXPERIMENTAL

Chemicals. 5-hydroxymethylfurfural (HMF), (99.9%, Acros Organics), formyl furan carboxylic acid (FFCA) (96%, Chemie Brunschwig AG), diformyl furan (DFF) (98%, TCI Europe N.V), hydroxymethylfuran carboxylic acid (HFCA) (95%, Apollo Scientific), 2,5-furandicarboxylic acid (FDCA) (98%, Chemie Brunschwig AG), and $Ni(NO_3)_2{\cdot}6H_2O$ (99.99%, Sigma Aldrich) were purchased and used without further purification. All organic chemicals were stored in a refrigerator.

Electrolytes. LiOH (99.995%, Sigma Aldrich), CsOH (99.9% trace metal basis, 50 wt% solution, Acros Organics), NaOH (99.99%, Fisher Scientific) and KOH (99.99% semiconductor grade, trace metal basis, Sigma Aldrich).

NiO-OH-Electrode Preparation. Fluorine-doped tin oxide (FTO) TEC 15 (12 - 14 Ω/square) from Pilkington was used as substrate, which was thoroughly cleaned by ultrasonic sonication for 10 minutes sequentially with soapy water (Deconex), deionized water, acetone, and finally isopropanol. To improve the electrical contact between the FTO and the cabling an ultrasonic soldering was used. The $Ni(OH)_2$

thin films were electrodeposited by chronoamperometry (with a Bio-Logic SP-150 potentiostat). A constant voltage of –900mV vs Ag/AgCl was applied to the FTO in a stirred solution containing 100 mM $Ni(NO_3)_2 \cdot 6H_2O$ and a charge of 5 mC/cm^2 was passed.[1] For a conversion of 2 e^- to one $Ni(OH)_2$ we would expect for 4 cm^2 (20 mC with 5 mC/cm^2) 104 nmol of nickel or 26 nmol/cm^2. It has also been reported that due to direct nitrate reduction (from the $Ni(NO_3)_2$ precursor salt in the solution) out of 8 e^- even 10 OH^- can be formed which would lead to a possible maximum nickel concentration of 130 nmol on a 4 cm^2 surface electrode (see also actual detection of nickel and iron with ICP-MS below and Table S 1).[3–7]

2 electron with 1 Ni process (Ref. 2):

$$2\ H_2O + 2e^- \longrightarrow H_2 + 2\ OH^-$$

$$Ni^{2+} + 2\ OH^- \longrightarrow Ni(OH)_2$$

8 electron with 5 Ni process (Ref. 3):

$$NO_3^- + 7\ H_2O + 8\ e^- \longrightarrow NH_4^+ + 10\ OH^-$$

$$5\ Ni^{2+} + 10\ OH^- \longrightarrow 5\ Ni(OH)_2$$

The calculated thickness is ~7 nm assuming a homogeneous deposition and 100 % faradaic efficiency using two electron process (2 electrons form one $Ni(OH)_2$).[2] All the samples prepared for our experiments have a nearly equivalent amount of active Ni species on the electrode surface, as shown by the area of the nickel redox peaks in the CV scan.

The main catalytic species of the catalyst film is NiO-OH. The highest catalytic activities of NiO-OH for Oxygen evolution reaction (OER) are reported for potentials above 1.4 V vs RHE in strong basic media (pH 14).[8] Generally to achieve high catalytic activity of NiO-OH films, they have to be electrochemically activated. The activation of the nickel catalyst thin films was performed by cycling 50 times from 1 to 2 V vs RHE with a 50 mV/s scan rate (so that a reproducible anodic current was obtained and no change in the CVs was observed anymore). The electrochemical activation process under strong alkaline conditions allows for a surface reconstruction of $Ni(OH)_2$ species and thus reduces the energy

barrier for transformation of $Ni(OH)_2$ to NiO-OH.[9] The activated NiO-OH films were then used for the investigations.

Electrochemical Measurements. The electrolysis reactions were performed with a Bio-Logic SP-150 potentiostat in a single compartment electrochemical cell with 1 M aqueous alkali hydroxide solution (CsOH, KOH, NaOH, or LiOH) as supporting electrolyte (10 mL). The electrochemical cell consisted of cleaned Pt wire, the freshly prepared and activated NiO-OH film, and an Ag/AgCl reference electrode. The solutions were vigorously stirred during the reaction. The measured electrochemical potentials were converted to the RHE (reversible hydrogen electrode) scale by using the following equation:

$$E_{RHE} = E_{Ag/AgCl} + 0.059\ x\ \mathrm{pH} + \mathrm{E}^{0}_{\mathrm{Ag/AgCl}}$$

where $\mathrm{E}^{0}_{\mathrm{Ag/AgCl}}$ = 0.197 V (at 25 °C) is the standard potential of the Ag/AgCl (KCl sat) reference electrode, and $E_{Ag/AgCl}$ is the experimentally measured potential against the Ag/AgCl reference electrode. The CVs of HMF oxidation reaction (HMF-OR) and OER were recorded from 1 to 2 V vs RHE with a scan rate of 5 mV/s for three consecutive measurements and the last measurement was used for analysis.

The chronoamperometry of 5 mM HMF oxidation was performed by applying a constant potential of 1.5 V vs RHE, until a maximum of 29 coulombs were passed, with a maximum time of 20 hours (some reactions therefore did not achieve complete conversion of HMF to FDCA). CVs of HMF oxidation were recorded before and after chronoamperometry again with 5 mV/s.

The effect of iron incorporation into the NiO-OH films was investigated intentionally adding iron ($FeCl_2{\cdot}4H_2O$; 99.99% trace metal basis, Sigma Aldrich). 20 μl of a 25 or 50 μM stock solution was added to iron free electrolyte solution in the electrochemical cell. This equals the addition of 0.5 nmol or 1 nmol of iron. By electrodeposition 26 nmol of nickel atoms have been deposited onto the FTO surface

per cm^2 (assuming 100% faradaic efficiency). The total area of the electrode is 4 cm^2, therefore 104 nmol of nickel atoms were present in the electrode. The ratio of nickel to iron is 208 to 1 and 104 to 1.

Removal of Traces of Iron from the Electrolyte Solution. To purify the electrolyte solutions from iron impurities, we followed a previously reported procedure.[10,11] In a first step, nickel hydroxide particles were precipitated by addition of $Ni(NO_3)_2 \cdot 6H_2O$ (2 g) to the 1 M alkali metal hydroxide electrolyte solution to be cleaned (10 ml). The mixture was dispersed by sonication for 10 minutes, the precipitate was separated by centrifugation (2500 rpm, 30 min), and the supernatant was decanted. The $Ni(OH)_2$ precipitate was washed five times by dispersing in fresh electrolyte solution, centrifuging and decanting the supernatant. The resulting high surface area $Ni(OH)_2$ precipitate was then used as an iron absorbent. It was added to 30 ml of electrolyte solution to be purified, agitated vigorously for 10 min and stored for 3 hours. After centrifugation (2500 rpm, 30 min), the supernatant solution could be used as an iron-free electrolyte solution for electrochemical experiments. The same procedure was followed for each electrolyte solution separately.

Ultrahigh-Pressure Liquid Chromatography (**UPLC) Procedure**. The HMF, FDCA and intermediates were quantified by reverse phase UPLC separation method. UPLC was performed on a Waters Acquity UPLC System, using an Acquity UPLC BEH C18 1.7 µm (2.1 x 50 mm) column. UPLC solvents were aqueous (0.1% trifluoroacetic acid in millipore water) (solvent A) and acetonitrile HPLC grade (solvent B). The flow rate was 0.6 ml/min and the solvent gradient was ramped from 95% aqueous to 95% organic over 6 minutes. A diode array detector was used to detect the eluents. The products were quantified by integrating the peak area in the absorption spectrum and comparing with a standard calibration curve which are presented in Figure S15.

Proton Nuclear Magnetic Resonance (^{1}H-NMR) Procedure. The ^{1}H-NMR spectra were recorded on a Bruker 300 MHz spectrometer. The analyzed solution contained 0.1 ml of reaction mixture and 0.4 ml of D_2O solvent, along with t-butanol (2 mM final concentration) as internal integration standard

(99.99%, Sigma Aldrich). For the *in-situ* HMF degradation studies and standards for the intermediate products, 1 M deuterated electrolyte solution was used. The quantification of the products may be prone to minor errors due to challenging baseline corrections as a result of the large amount of water in the spectra.

Energy-dispersive X-ray spectroscopy. EDX analysis was performed by using Zeiss Supra 50 VP scanning electron microscope.

Atomic Force Microscopy. An Asylum Research AFM (MFP-3D) was used to measure the surface morphology in tapping mode. The probe used for the measurement was a HQ:NSC15/Al BS from MikroMasch. The Asylum Research built in software was used to further analyze the AFM pictures.

Inductively Coupled Plasma Mass Spectroscopy (ICP-MS) for the determination of the amount of electrodeposited nickel and the content of iron in the HMF stock solution. The ICP-MS were used to quantify iron in the stock solution of HMF and the amount of electrochemically deposited Ni on the FTO surface. The measurements were performed on an Agilent QQQ 8800 Triple quad ICP-MS Spectrometer (Agilent technologies Switzerland) with an ASX200 autosampler (Agilent technologies Switzerland), equipped with standard nickel cones and "micro – mist" quartz nebulizer fed with 0.3mL / minute analytic flow.

ICP-MS to detect the amount of nickel deposited: Two samples of deposited nickel species were investigated. For the ICP-MS the deposited nickel salt on FTO (area 4 cm^2) was dissolved in 2% ultrapure HNO_3. The samples were left in the acidic solution for 48h to dissolve all of the nickel salt. In average we have determined 126 nmol of nickel for the two samples measured. To cross-check if any of the nickel salt remained on the FTO surface after HNO_3 etching, the samples were measured afterwards by CV in 1 M aqueous LiOH solution. No further nickel oxyhydroxide oxidation peaks were detected showing that all the nickel has been dissolved in the 2% HNO_3.

ICP-MS of HMF to detect its Fe content: 87.059 mg of HMF was dissolved in 60% ultrapure HNO_3. For the 87.06 mg of HMF, 17 ng of iron species were detected by ICP-MS. The electrolyte compartment of the measurement cell contained 10 mL of 5 mM HMF solution corresponding to 6.31 mg of HMF. In total 1.23 ng of iron (0.022 nmol) is present in the 10 ml electrolyte compartment originating from the HMF stock.

Calculation of the nickel to iron ratio. If we consider the two electron process (please see the **NiO-OH-Electrode Preparation** process at the beginning of the experimental part) of nickel deposition for the following calculation as this yields the minimum possible ratio of nickel to iron. We have deposited at least 104 nmol (26 nmol/cm^2) nickel on to the 4 cm^2 FTO electrode surface. The electrolyte solution contains 1.23 ng of iron (0.022 nmol), which we assume it enters all into the nickel electrode matrix. This yields a nickel to iron ratio of 4700:1 meaning for one iron atom 4700 nickel atoms are present. Using the ICP-MS determined amount of 126 nmol for the nickel electrodes, the ratio would be even higher with 5700 nickel atoms to one iron atom. Calculated values for all nickel to iron ratio are showed in table S1.

X-ray photoelectron spectroscopy (XPS): XPS was performed using a Physical Electronics (PHI) Quantum 2000 Xray photoelectron spectrometer featuring monochromatic AlKα radiation, generated from an electron beam operated at 15 kV and 32.3 W. The energy scale of the instrument was calibrated using a Au reference sample. The analysis was conducted at 1×10 6 Pa, with an electron take off angle of 45° and a pass energy of 23.50 eV. Core level binding energies were determined by fitting Voigt profiles (GL30) after U 2 Tougaard background subtraction. Charge neutralization was used throughout the measurement.

2. FIGURES AND TABLES

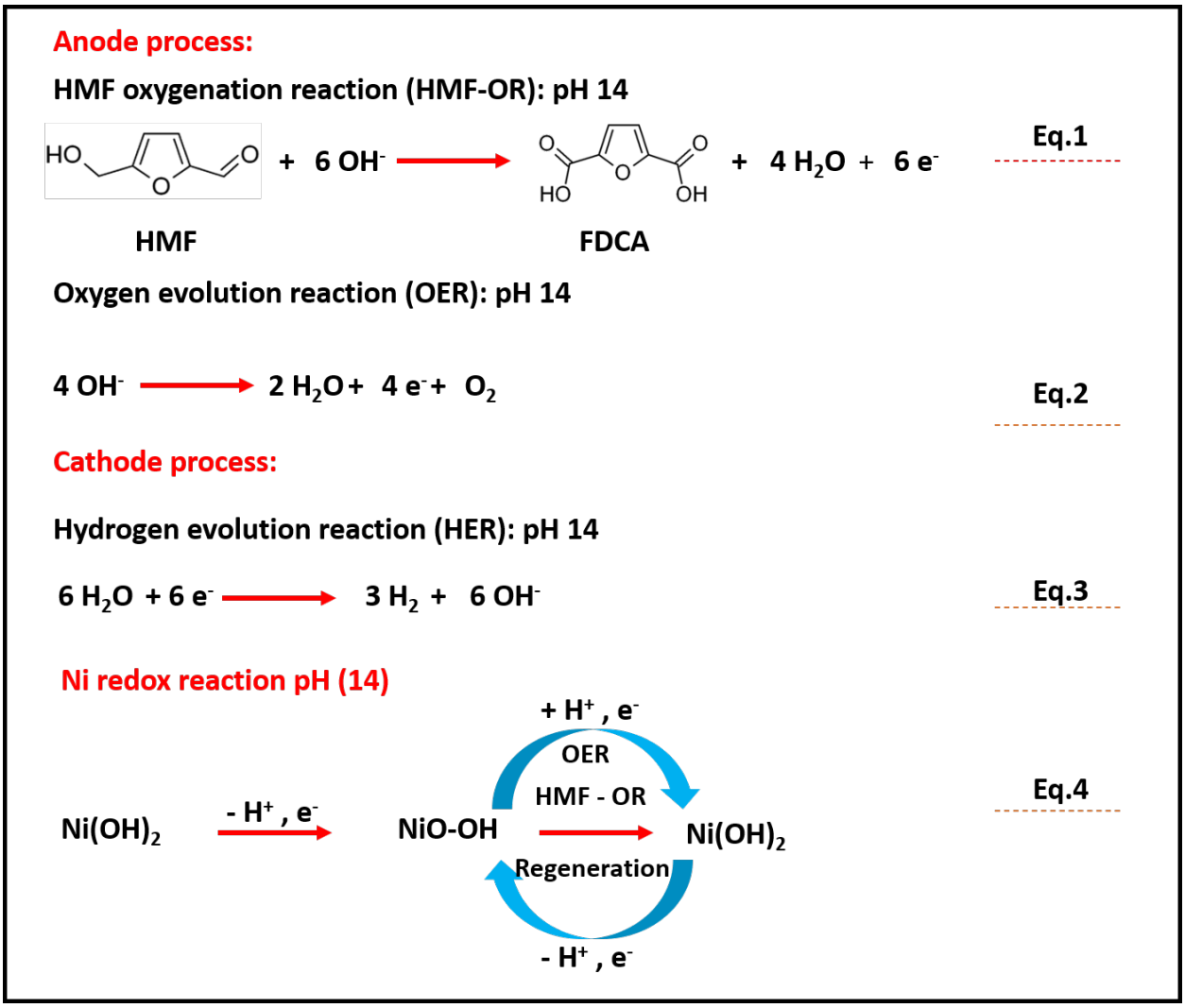

Fig S1. Redox reactions involved: HMF-OR, HER, OER and NiO-OH redox reactions.

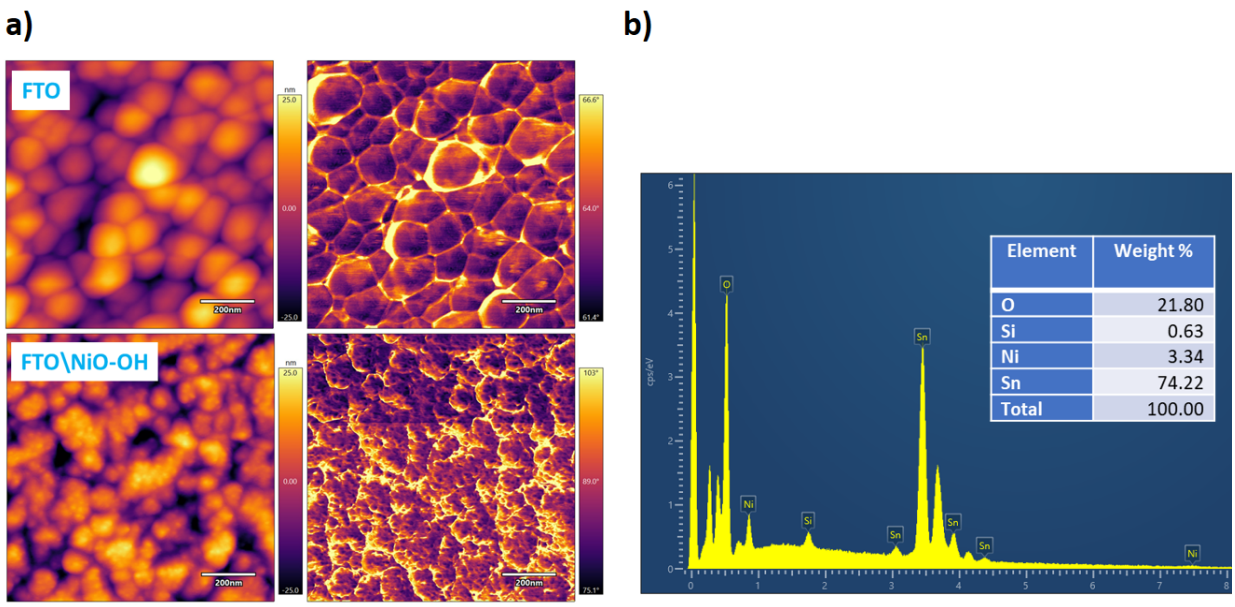

Fig S2. (a) Comparison of the FTO and the NiO-OH on FTO (after usage for HMF oxidation) by atomic force microscopy. Left images show the surface topography and right images show the phase shift of the cantilever during the AFM scan. Topography and phase shift show the different fine-structure on the FTO/ NiO-OH surface. (b) Energy dispersive X-ray analysis of NiO-OH thin films.

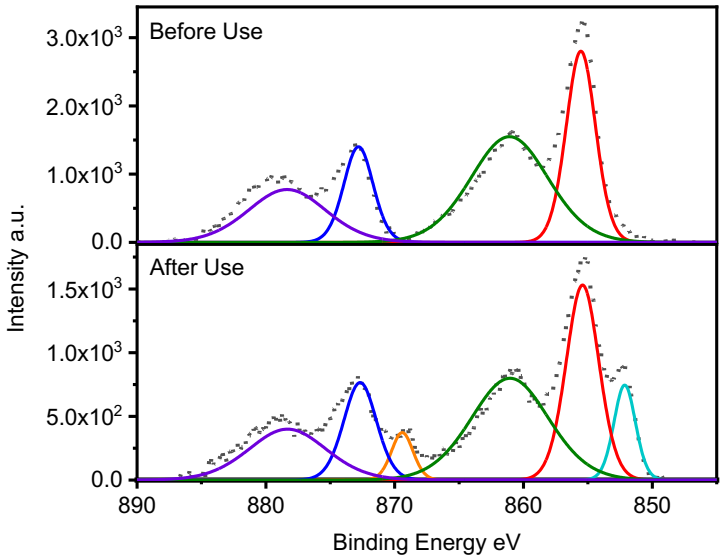

Fig S3. The electrodeposited $Ni(OH)_2$ film seen in the 'Before Use' XPS spectra shows components at 855 and 872 eV for Ni $2p_{3/2}$ and Ni $2p_{1/2}$ peaks, respectively, along with their respective satellite peaks, which correspond to the binding energy matching to Ni^{II} in the $Ni(OH)_2$ form. However, after electrochemical oxidation experiments, new components appear at lower binding energy, which indicates a mixture of Ni^{II} and Ni^{III} species.

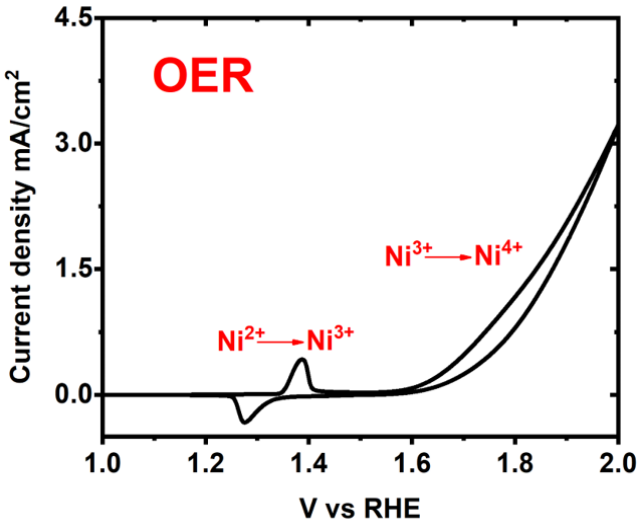

Fig S4. CV (under stirring) of OER on NiO-OH electrode, with assigned redox peaks. 1 M LiOH without iron in the electrolyte and a scan speed is 5 mV/s.

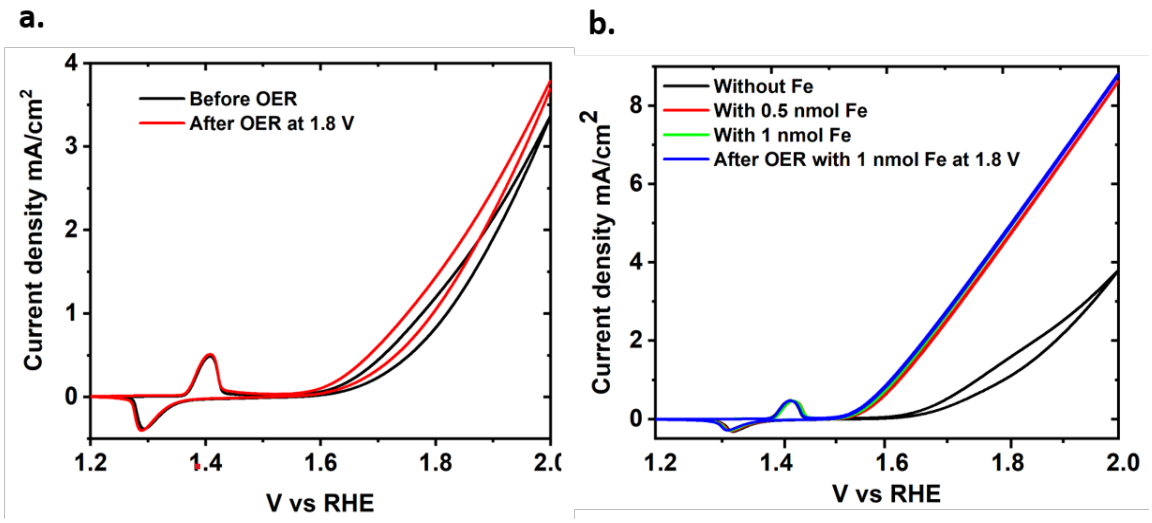

Fig S5. (a) CV of OER on a NiO-OH electrode, recorded before and after chronoamperometry in 1 M LiOH without iron in the electrolyte solution. (b) CV of OER on a NiO-OH electrode without iron present in the LiOH electrolyte solution, with intentionally added iron (nickel to iron ratio of 208 to 1 and 104 to 1) and after chronoamperometric measurement.

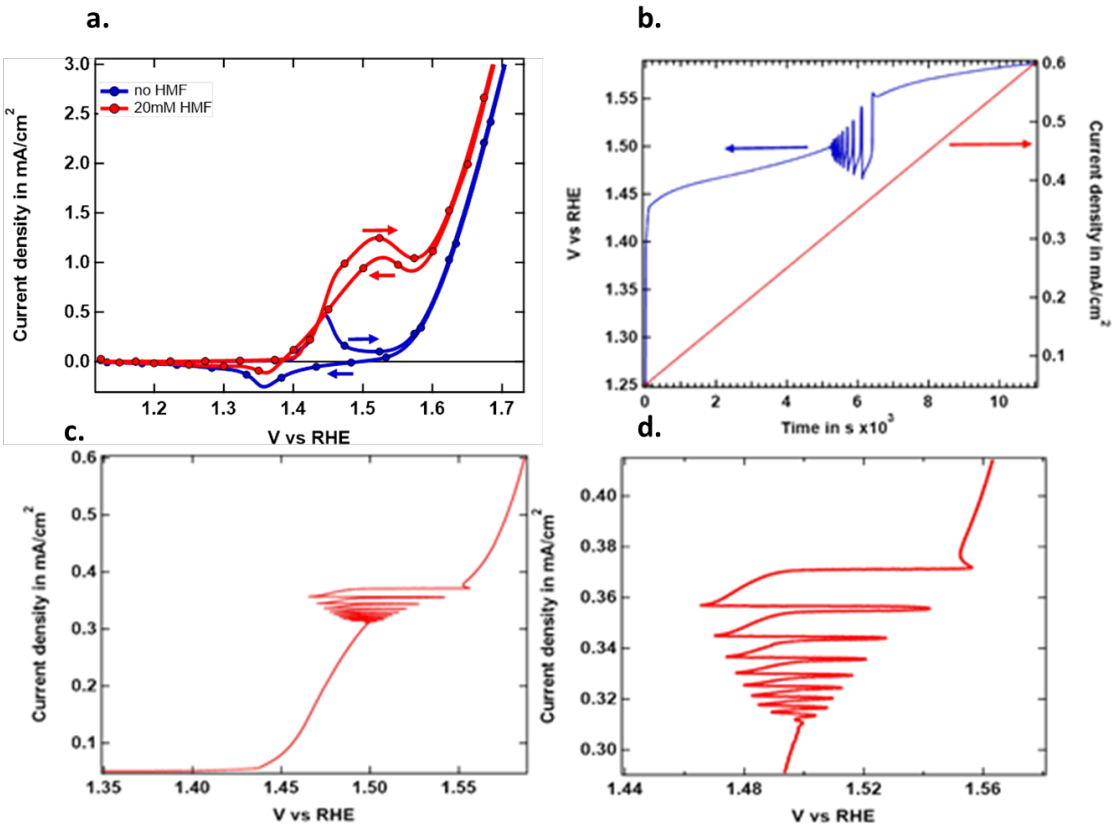

Fig.S6. (a) CV with 5 mV/s in 1 M LiOH with and without HMF (20 mM); (b) voltage and current during galvanodynamic scan with 50 nA/s with HMF; (c) current vs. voltage of the galvanodynamic scan in (b); (d) magnification of (c).

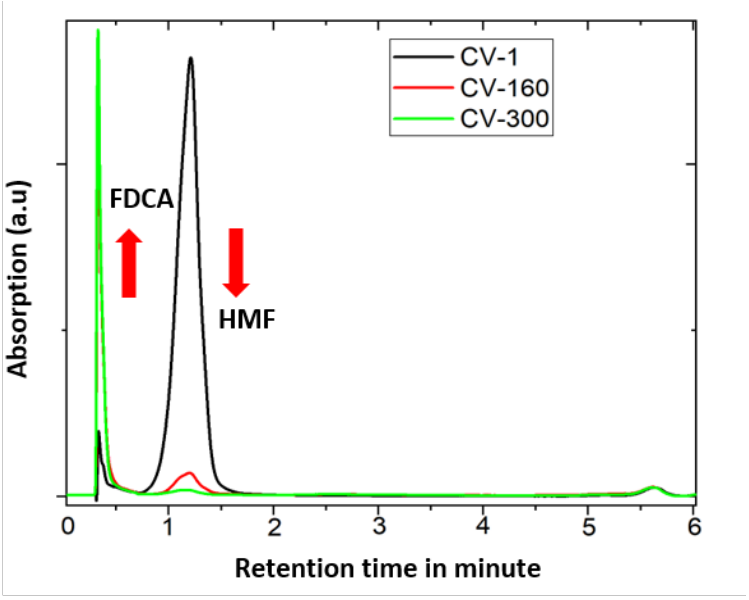

Fig S7. UPLC data of the HMF oxidation reaction mixtures, recorded with subsequent number of CV cycles. Note: the FDCA always eluted at the solvent front and the reaction was therefore also characterized by ^{1}H NMR to ensure correct interpretation.

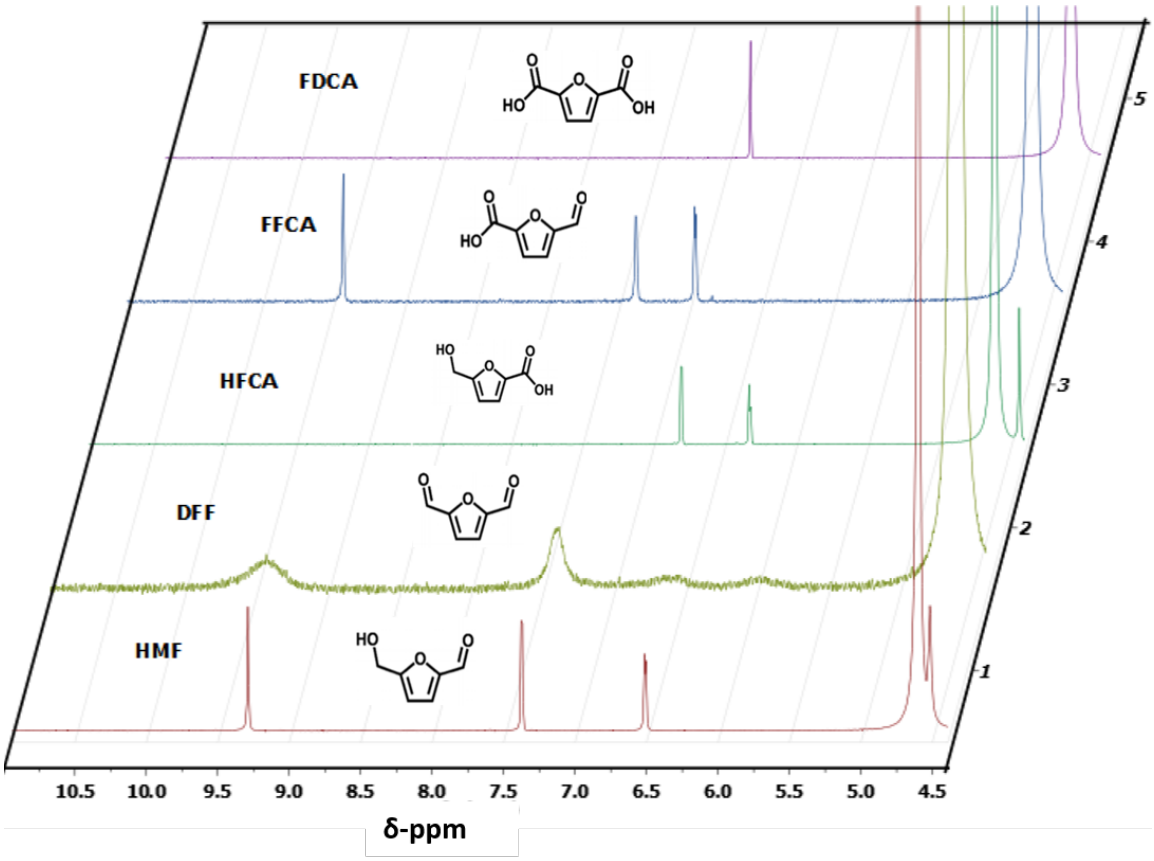

Fig S8. ^{1}H-NMR spectra of standard solutions of HMF and its intermediates recorded in 1 M LiOD electrolyte solution.

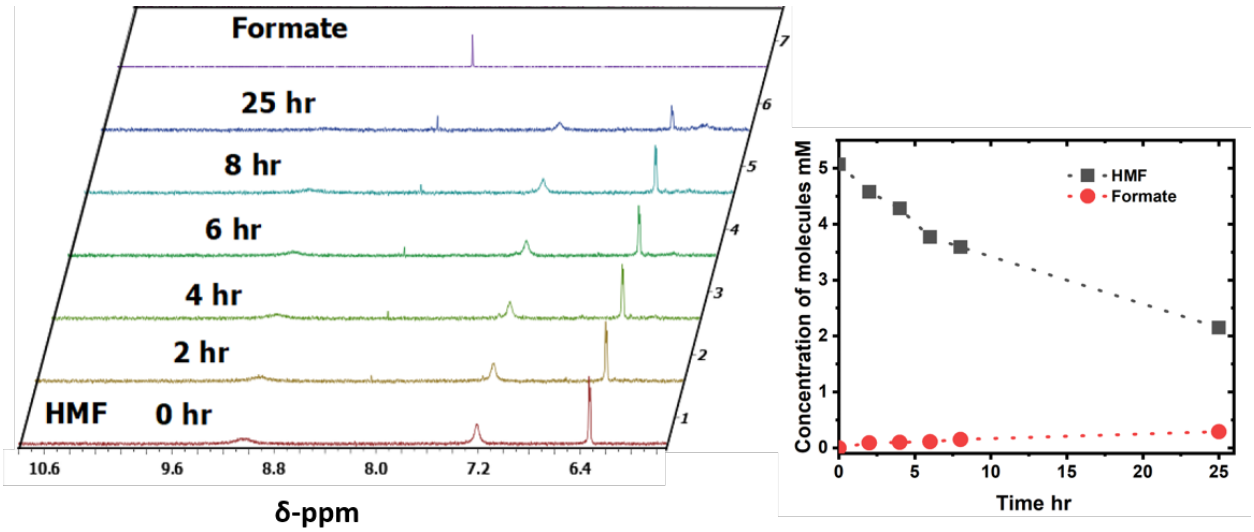

Fig S9. ^{1}H-NMR spectra of in situ HMF degradation over 25 hours measured at different intervals directly in the NMR tube with D_2O as solvent with 1 M LiOD electrolyte (left), and HMF concentration vs time quantified by integrating the HMF and formate peak from the ^{1}H-NMR (right).

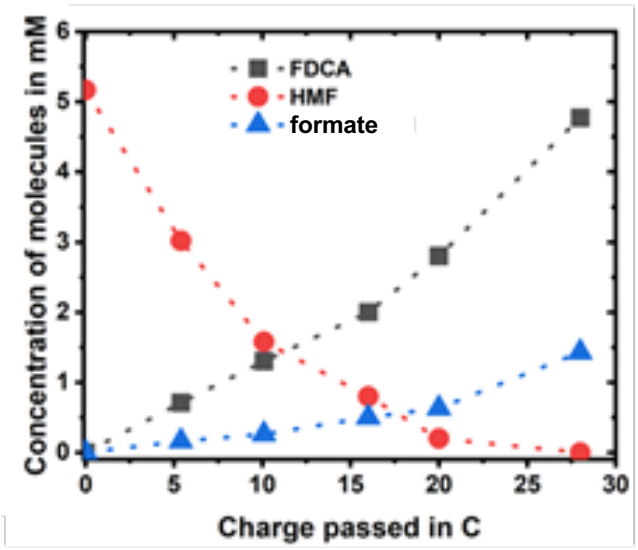

Fig S10. Concentrations of HMF, FDCA, and formate during the electrochemical HMF oxidation reaction.

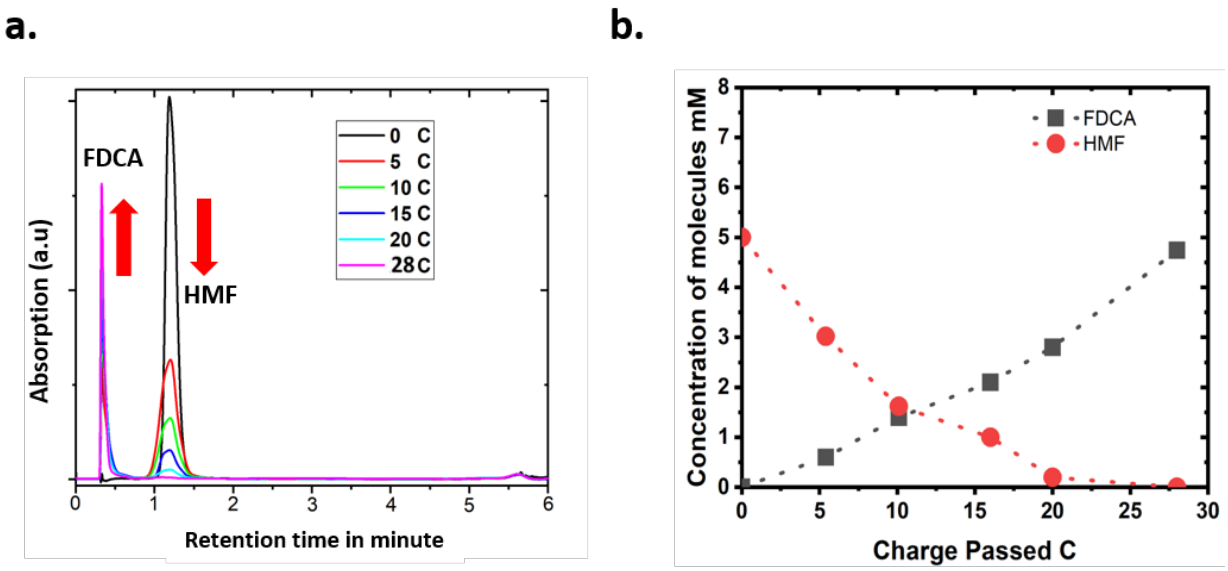

Fig S11. (a) UPLC data obtained from taking aliquots of the reaction mixture after 5 C of charge had passed during the electrolysis (in 1 M LiOH solution). Note: the FDCA always eluted at the solvent front and the reaction was therefore also characterized by ^{1}H-NMR to ensure correct interpretation. (b) the concentration of HMF consumed and FDCA formed during electrochemical HMF oxidation reaction. The final data point at ~28 C was obtained after stopping the electrolysis and equilibrating the electrolyte solution under stirring for 5 min in the absence of an applied potential. The formate is remain undetected in the separation column due to its absorption wavelength, which is off range in the UPLC detector.

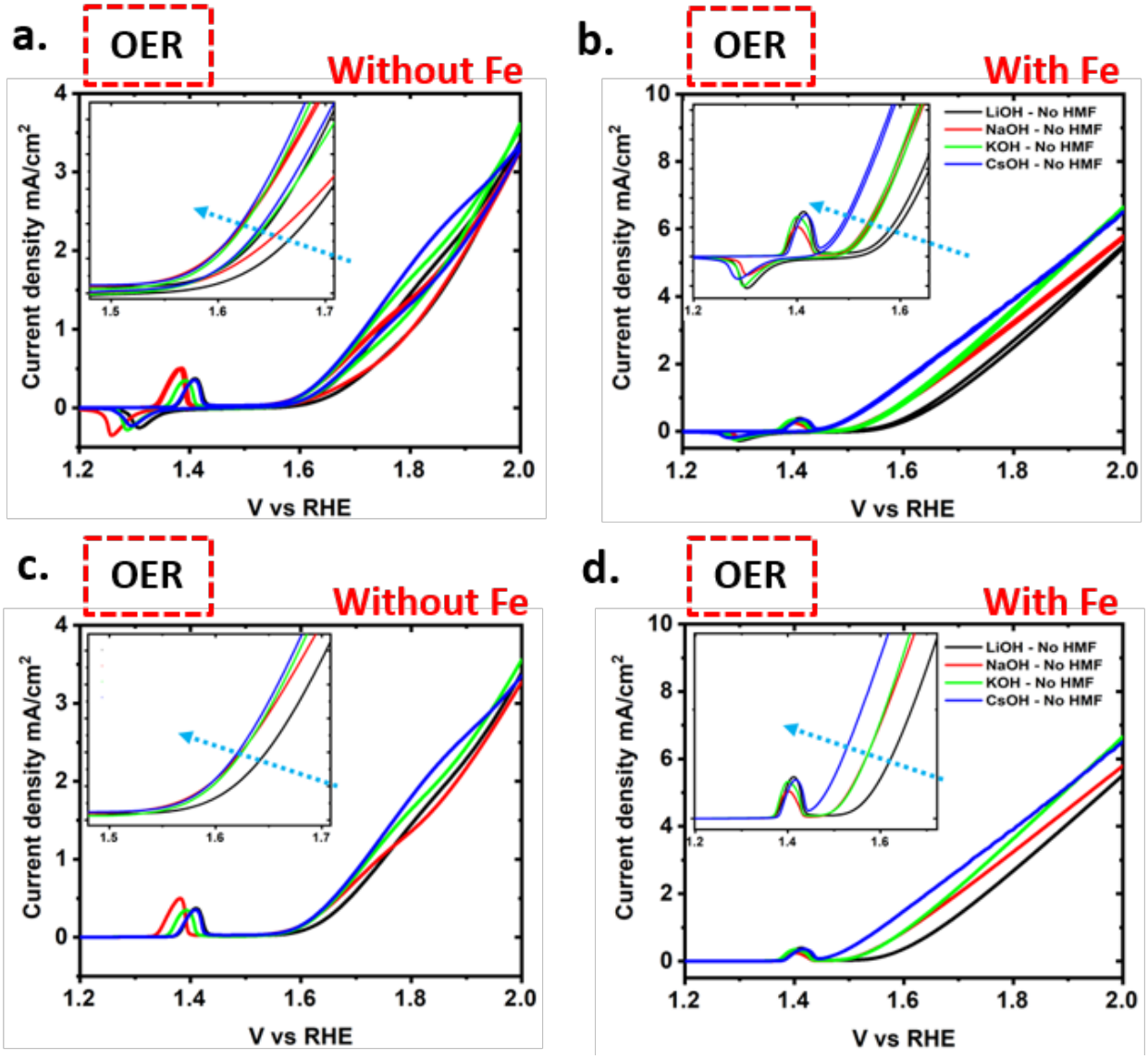

Fig S12. (a) and (b) present the CVs of OER reactions on NiO-OH electrodes with different 1 M alkali hydroxide and without and with iron in the electrolyte solution, respectively. (c) and (d) are the only forward polarization curve of the same.

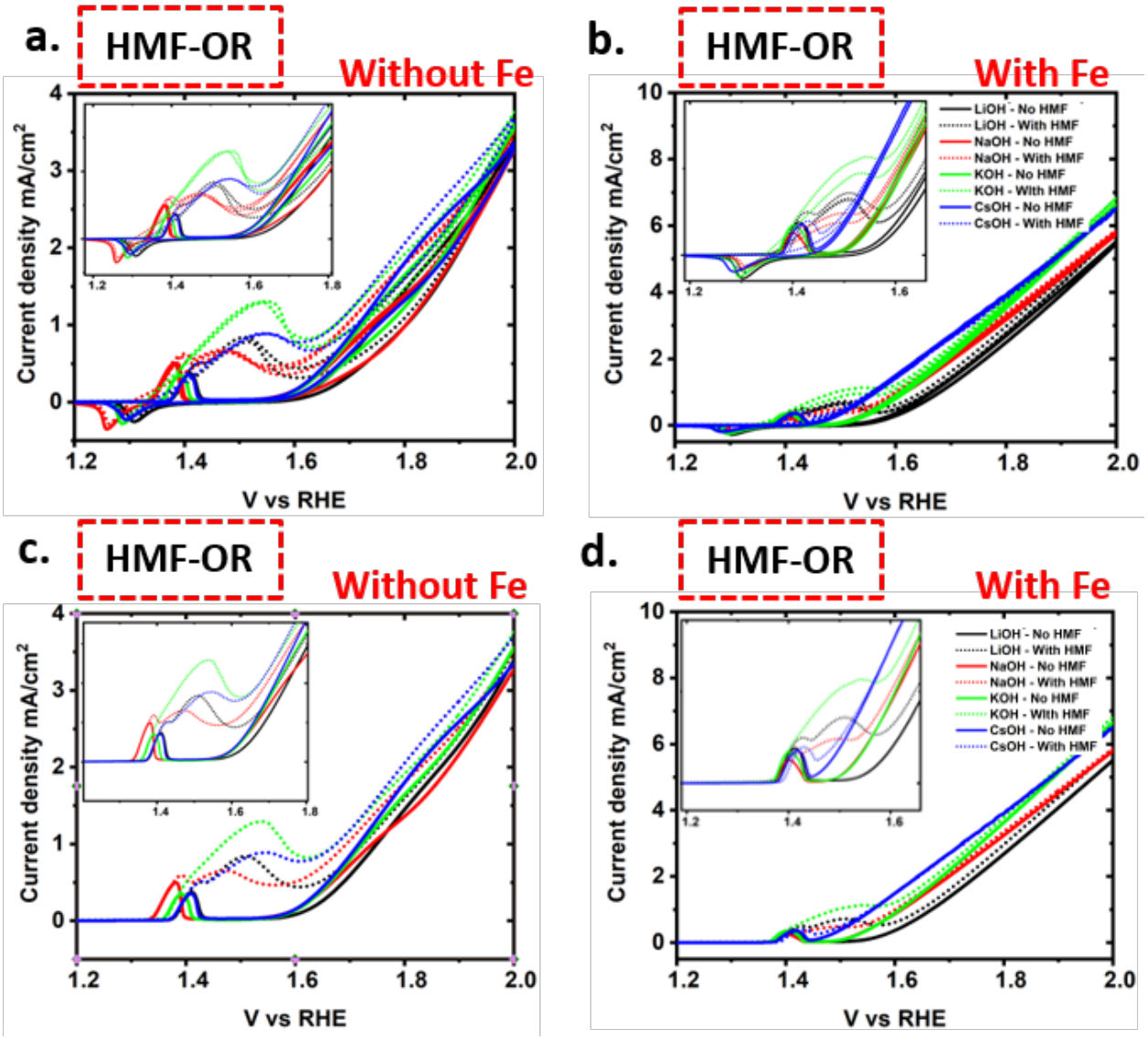

Fig. S13. (a) and (b) present the CVs of HMF oxidation reactions and OER on NiO-OH electrodes with different 1 M alkali hydroxide and without and with iron in the electrolyte solution, respectively. (c) and (d) are the only forward polarization curve of the same.

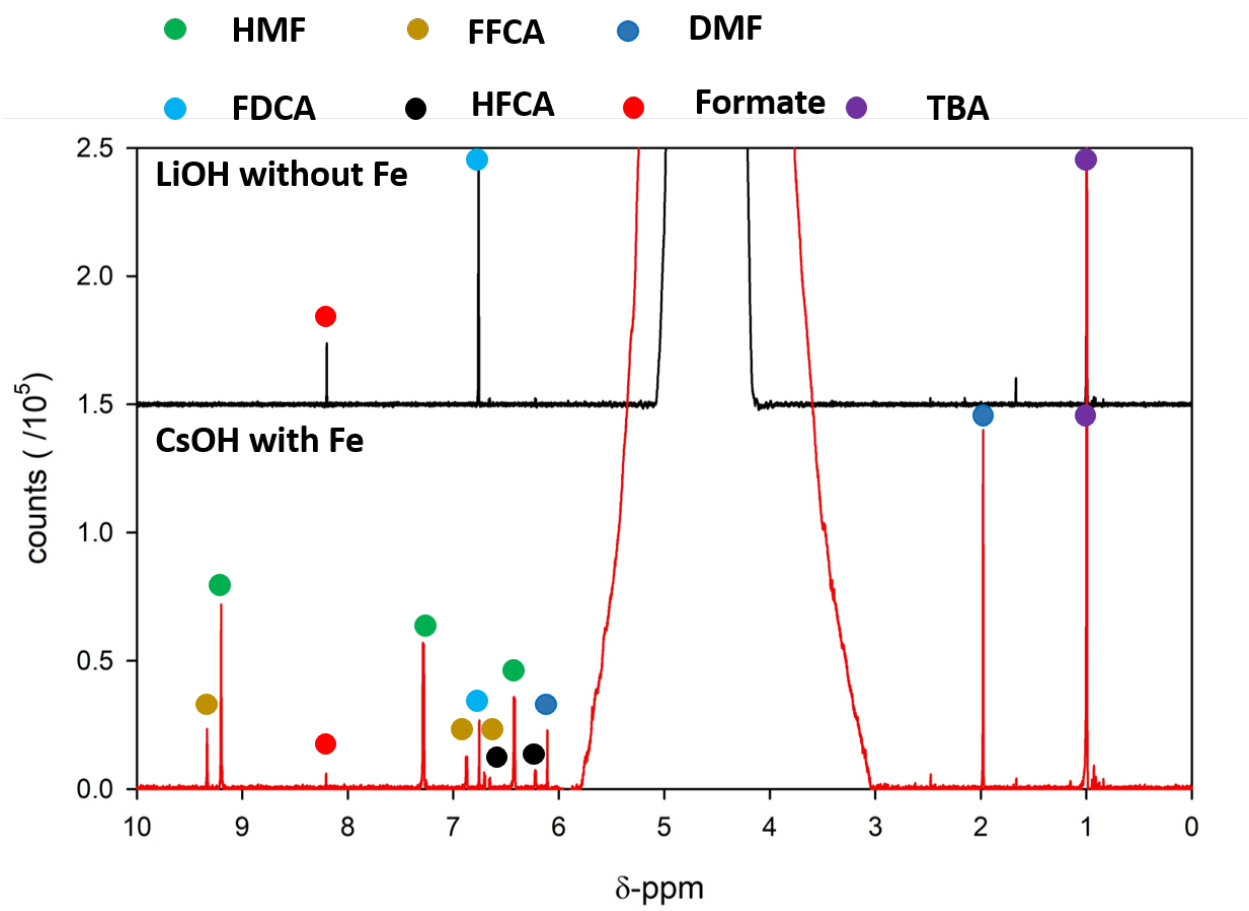

Fig S14. ^{1}H-NMR spectra of the HMF oxidation reaction (OR) mixture comparing the best (LiOH, without iron) and worst (CsOH, with iron) catalytic conditions. The large peak at 4.6 δ-ppm corresponds to water. The abbreviations written in the above figures are DMF (2,5-Dimethylfuran),[12] HMF (5-Hydroxymethylfurfural), FDCA (2,5-Furandicarboxylic acid), HFCA (Hydroxymethylfuran carboxylic acid), FFCA (Formylfuran carboxylic acid), Formate, and TBA (T tert- Butyl alcohol).

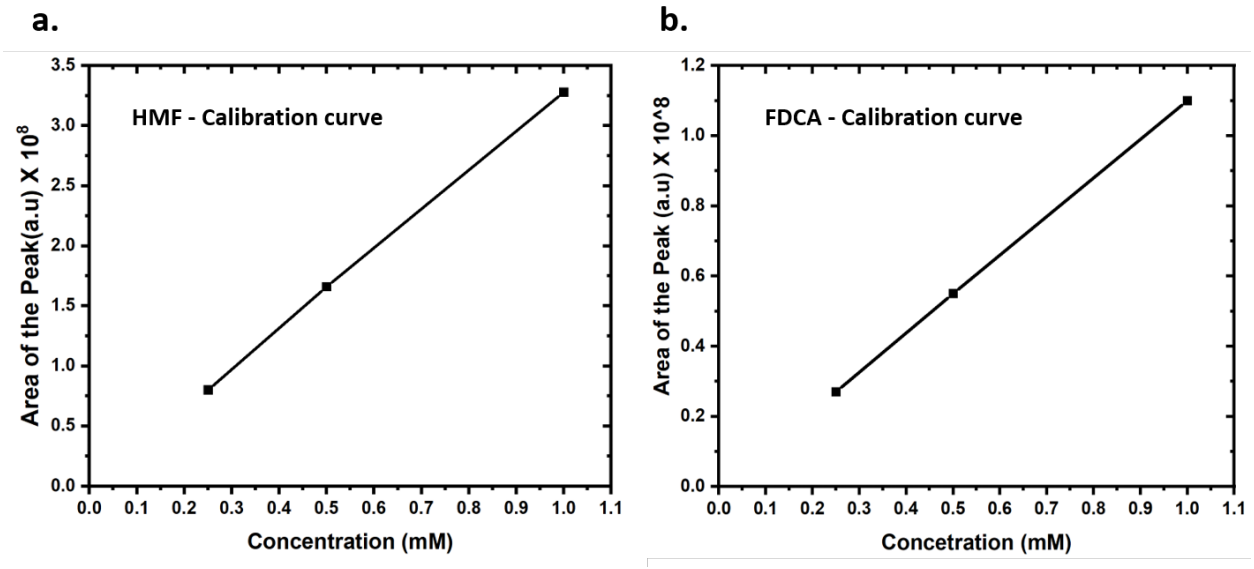

Fig S15. a) HMF b) FDCA UPLC calibration curve used for analysis and quantification of reaction mixtures.

Faradaic Efficiency Calculations

$$\text{FE (\%)} = \frac{Charge\ used\ for\ FDCA\ production}{Total\ charge\ passed}\ x\ 100$$

$$\text{FE (\%)} = \frac{Mol\ of\ FDCA\ formed\ \text{x}\ (6\ \text{x}\ F)}{Total\ charge\ passed}\ x\ 100$$

F= Faraday constant= 96485 C mol^{-1}

Chemical Yield Calculations

Initial moles of HMF is 5mM

$$\text{CY (\%)} = \frac{Moles\ of\ FDCA\ formed}{Initial\ moles\ of\ HMF}\ x\ 100$$

Table S1. Comparison of the two- and eight-electron nickel deposition process with the IPC-MS results and the determined nickel-to-iron ratio.

	nmol of nickel on a 4 cm^2 FTO electrode	Iron content in stock solution (10 ml of 5mM HMF)	Nickel to Iron ratio
Two electron to one nickel process	104 (theoretical)	0.022	~4700:1
Eight electron to five nickel process	130 (theoretical)	0.022	~5900:1
ICP-MS measured	126	0.022	~5700:1

Table S2. The calculated Faradaic efficiency and yield for FDCA by UPLC method

Electrolyte	Condition	FDCA Concentration (mM)	Total charge Passed (C) at 1.5 V vs RHE	Faradaic Efficiency for FDCA (%)	Chemical Yield (%)
LiOH	Without iron	4.75	28	98	95
NaOH	Without iron	4.44	27	95	89
KOH	Without iron	4.35	27	93	87
CsOH	Without iron	3.54	22	93	71
LiOH	With iron	3.58	23	90	71
NaOH	With iron	4.41	29	88	88
KOH	With iron	4.26	29	85	85
CsOH	With iron	0.3	29	6	6

Table S3. Reaction mixture analysis from ^{1}H-NMR of HMF oxidation performed at 1.5 vs RHE with best catalytic condition (LiOH, without iron) and most unfavorable catalytic condition (CsOH, with iron) after chronoamperometry.

Compound	1M LiOH without iron: Concentration of Product (mM)	Faradaic Efficiency for FDCA %	1M CsOH with iron: Concentration of Product (mM)	Faradaic Efficiency for FDCA %
HMF	0		2.8	
FDCA	4.77	99%	0.35	6%
Formate	1.38		0.15	
FFCA	0		0.75	
HFCA	0		0.53	
Dimethylfuran	0		0.46	

3. NOTE: regarding the FE

FE is related to the amount of charge passed through the electrode that is used to oxidize HMF to FDCA during the reaction. This means that in our experiment with highest FE of 99%, a 99% of the charge passed through the electrodes are used to produce FDCA and only 1% goes to side reactions. Also, 99% of FE does not means 99% chemical yield of FDCA from HMF. Chemical yield is calculated from the initial concentration of HMF. In fact, in our case we have highest 95% yield of FDCA from HMF for solution with Li cation (iron free) solution (Table S1). The other 5% of HMF has been transformed in formate as a degradation product without the application of potential as shown in Figure S7. Our claims match very well with the ^{1}H-NMR data in Figure 3, showing only FDCA and formate signals.

REFERENCES:

1 G. R. Fu, Z. A. Hu, L. J. Xie, X. Q. Jin, Y. L. Xie, Y. X. Wang, Z. Y. Zhang, Y. Y. Yang and H. Y. Wu, *Int. J. Electrochem. Sci.*, 2009, **4**, 1052–1062.

2 R. S. Jayashree and P. V. Kamath, *J. Power Sources*, 2001, **93**, 273–278.

3 P. E. Sharel, D. Liu, R. A. Lazenby, J. Sloan, M. Vidotti, P. R. Unwin and J. V. Macpherson, *J. Phys. Chem. C*, 2016, **120**, 16059–16068.

4 M. Aghazadeh and M. R. Ganjali, *J. Mater. Sci. Mater. Electron.*, 2017, **28**, 8144–8154.

5 R. Kostecki and F. McLarnon, *J. Electrochem. Soc.*, 1997, **144**, 485–493.

6 C. C. Streinz, S. Motupally and J. W. Weidner, *J. Electrochem. Soc.*, 1995, **142**, 4051–4056.

7 M. Wei, Q. Huang, Y. Zhou, Z. Peng and W. Chu, *J. Energy Chem.*, 2018, **27**, 591–599.

8 O. Diaz-Morales, D. Ferrus-Suspedra and M. T. M. Koper, *Chem. Sci.*, 2016, **7**, 2639–2645.

9 J. Huang, Y. Li, Y. Zhang, G. Rao, C. Wu, Y. Hu, X. Wang, R. Lu, Y. Li and J. Xiong, *Angew. Chemie - Int. Ed.*, 2019, **58**, 17458–17464.

10 A. C. Garcia, T. Touzalin, C. Nieuwland, N. Perini and M. T. M. Koper, *Angew. Chemie*, 2019, **131**, 13133–13137.

11 B. J. Taitt, D. H. Nam and K. S. Choi, *ACS Catal.*, 2019, **9**, 660–670.

12 SDBSWeb : http://sdbs.riodb.aist.go.jp (National Institute of Advanced Industrial Science and Technology, September 8, 2014), SDBS Number - 10444.